Rheology of a Low-Filled Polyamide 6/Montmorillonite Nanocomposite

Guangyang Xu,[1,2] Guangming Chen,[1] Yongmei Ma,[1] Yucai Ke,[1] Minfang Han[2]

[1]*Beijing National Laboratory for Molecular Sciences (BNLMS), Laboratory of New Materials, Institute of Chemistry, Chinese Academy of Sciences, Beijing, China 100080*
[2]*School of Chemical and Environmental Engineering, China University of Mining and Technology, Beijing, China 100083*

Received 16 May 2007; revised 20 November 2007
DOI 10.1002/app.27750
Published online 25 January 2008 in Wiley InterScience (www.interscience.wiley.com).

ABSTRACT: The rheological properties of a polyamide 6/clay nanocomposite with a low loading of clay (1 wt %) were studied. Linear viscoelastic measurements in oscillatory and steady shear with small strain amplitudes were carried out. The nanocomposite exhibited a higher elastic modulus, viscous modulus, and complex viscosity than neat polyamide 6 during dynamic and steady shear tests. Moreover, the addition of clay resulted in a reduction of the critical strain amplitude, an increase of the loss angle, and a reduction of the frequency at the intersection of the elastic and viscous moduli. © 2008 Wiley Periodicals, Inc. J Appl Polym Sci 108: 1501–1505, 2008

Key words: clay; composites; nanolayers; polyamides; rheology

INTRODUCTION

In the last 2 decades, polymer/clay nanocomposites (PCNs) have attracted much interest not only because of their dramatically increased physical and mechanical properties but also because of their particular nanostructures. In PCNs, highly anisotropic layered particles with a thickness of less than 100 nm and/or individual layers are homogeneously dispersed in a polymer matrix. In comparison with the large number of studies of the preparation and properties of PCNs, rheological investigations are relatively limited, although rheology is an effective tool in the study of the structure and structural changes of polymer/inorganic composites in molten and solution states. It has been found that the rheological behaviors of the molten state of poly(butylene terephthalate)/clay,[1] polyamide 12/clay,[2–4] copolyamide/clay,[5] polypropylene/clay,[6] and polystyrene/clay[7] nanocomposites and the solution state of poly(ethylene oxide)/clay nanocomposites[8] are obviously different from those of their corresponding neat polymer resins. As for polyamide 6 (PA6)/clay nanocomposites, most reports have concentrated on rheological studies with clay loadings higher than 2 wt %.[9–14] For example, Wan et al.[9] studied the strain amplitude response of PA6/clay nanocomposites in both molten and solution states. Tung et al.[10] found that an *in situ* polymerized PA6/clay nanocomposite had a higher melt viscosity and higher tensile ductility than one prepared by melt blending, and this was attributed to the improved extent of dispersion and stronger interactions between the clay and polymer. Shen et al.[12] related the rheological behavior of PA6/attapulgite nanocomposites to their percolated structure.

In polymer nanocomposites, because the inorganic particles are dispersed on a nanometer scale, their rheological behaviors even at very low inorganic loadings should be obviously different from those of the corresponding neat polymer. Unfortunately, no detailed study of the rheological behavior for PA6/clay nanocomposites that focused on low clay loadings, such as 1 wt %, was found in our literature survey. In the literature,[9] the dependence of the elastic modulus (G') and viscous modulus (G'') on strain has been presented for PA6/clay nanocomposite containing 1 wt % clay. Ayyer and Leonov[14] reported that dynamic frequency sweep data of G' and G'' of a PA6/clay nanocomposite containing 1 vol % clay were different from those of the neat PA6 matrix. However, the viscosity data of the oscillatory rheometry and the steady shear rheology have not been reported up to now. Therefore, further detailed investigations of the rheology of PA6/clay nanocomposites with low clay loadings are necessary.

In this article, we mainly focus in detail on the oscillatory and steady shear rheological behavior of a low-clay-loaded PA6/clay nanocomposite. Here

Correspondence to: G. Chen (chengm@iccas.ac.cn) or Y. Ma (maym@iccas.ac.cn).

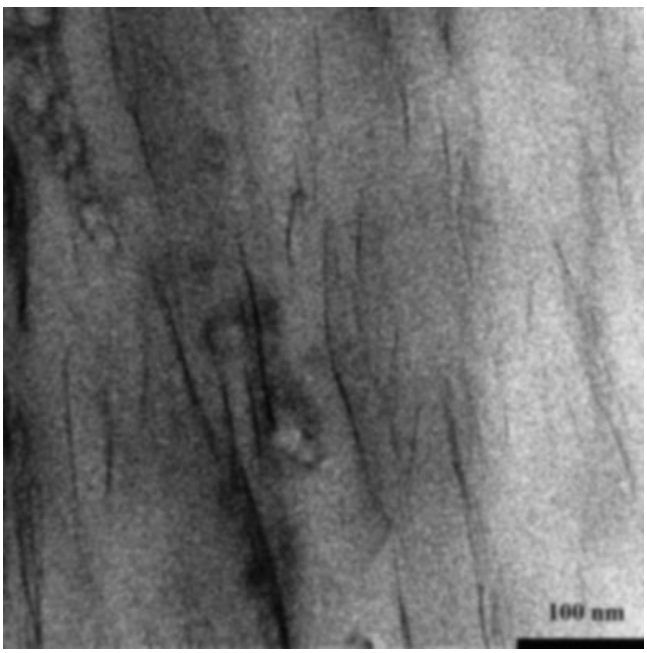

Figure 1 TEM image of a PA6/clay nanocomposite.

we chose a PA6 nanocomposite containing 1 wt % montmorillonite (MMT), which is called PA1. Its rheological data were systematically studied and compared with those of neat PA6 to study the effect of nanometer-scale dispersed clay particles.

EXPERIMENTAL

Materials

Two systems, PA1 (PA6/MMT nanocomposites containing 1 wt % MMT) and PA0 (the corresponding neat PA6), were chosen for this study. Both materials were generously provided by Baling Petro-Chemical Co., Ltd. (Yue Yang City, China), and were synthesized by the *in situ* intercalative polymerization method. The viscous average molecular weight of the polymer matrix for both materials was approximately 22,000. The clay used here was sodium montmorillonite (Na-MMT) with a cation-exchange capacity of about 100 mmol/100 g; it was kindly provided by Zhangjiakou Qinghe Chemical Factory (Zhangjiakou City, China).

Wide-angle X-ray diffraction (WAXD)

WAXD patterns were collected with a Rigaku (Tokyo, Japan) D/MAX 2500 X-ray diffractometer with Cu Kα radiation (λ = 0.154 nm) measured at room temperature. The scanning rate was 8°/min. The tube voltage and current were 40 kV and 200 mA, respectively.

Transmission electron microscopy (TEM)

TEM images were obtained with a Hitachi (Hitachi, Japan) H-800 transmission electron microscope operated at an acceleration voltage of 100 kV. Ultrathin samples of less than 100 nm were used.

Rheological tests

The rheological behavior was determined on a Gemini RH2000 rheometer (USA). In all the rheological testes, a pair of parallel plates with a diameter of 25 mm and a gap size of 1 mm were adopted. All measurements were conducted in a high-purity nitrogen atmosphere to prevent oxidative degradation. The injection-molded sample disks were used for measurements at 240°C after drying at 100°C for 24 h to prevent moisture-induced degradation of PA6.

Strain sweep experiments were carried out from 0.1 to 100% at an angular frequency (ω) of 1 rad/s. Dynamic sweep and steady shear rate tests were performed at a strain of 3% and at shear rate ranges of 0.1–500 rad/s and 0.003–10 s^{-1}, respectively.

RESULTS AND DISCUSSION

The exfoliation and dispersion state of MMT in the PA6 matrix are shown in Figures 1 and 2. It is obvious from the TEM image (Fig. 1) that the clay particles have been dramatically exfoliated into a nanometer scale with a primary particle thickness of less than 20 nm and homogeneously dispersed in the polymer matrix. The WAXD pattern of PA1 in Figure 2 exhibits an absence of a distinct, sharp diffraction peak with a 2θ angle lower than 10°. This suggests that the clay has been dramatically exfoliated. In addition, the diffraction peak of 2θ = 21° results from the γ-crystalline phase of PA6.

Figure 3 shows the strain sweep curves of G' of PA0 and PA1 at ω = 1 rad/s. In Figure 3(A), it is obvious that G' has a transition from linear to

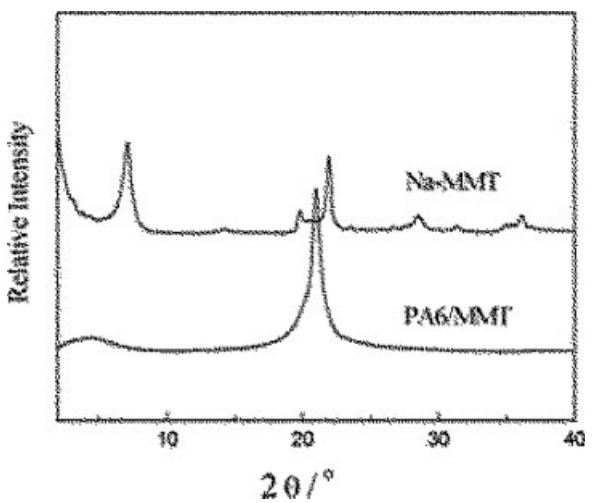

Figure 2 WAXD patterns of (A) Na-MMT and (B) a PA6/MMT nanocomposite containing 1 wt % MMT.

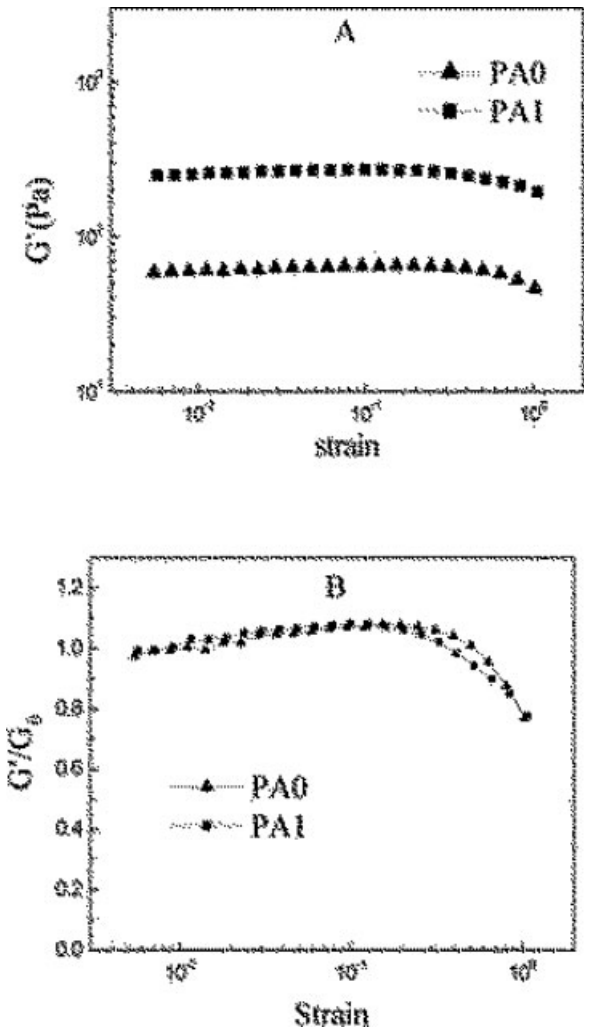

Figure 3 Strain amplitude dependence of (A) G' and (B) G'/G_0 for PA1 and PA0 measured at 240°C.

nonlinear viscoelastic behavior. To clearly observe the critical strain amplitude transition, the normalized elastic modulus (G'/G_0) from the values in the linear region at a low strain amplitude is shown in Figure 3(B). The critical transition is about 25% strain for PA1, which is obviously lower than that of PA0, about 38%. This behavior of a reduced critical strain transition of G' for PA1 versus PA0 for the low clay loading of 1 wt % is similar to the results of Wan et al.[9] In their study, the critical strain amplitude decreased from 18% for neat PA6 to about 15% for PA1. Both studies confirm that in the molten state, the critical strain amplitude is sensitive to clay addition and decreases logarithmically with the addition of clay even at a low clay loading of 1 wt %. Furthermore, the dependence of G'' on the strain amplitude is shown in Figure 4. The curves of G'' with the strain amplitude are similar to those deduced from G'. The critical strain amplitude measured from the normalized viscous modulus (G''/G_0) in Figure 4(B) is obviously larger than the value of 100% for PA0. It is interesting that the critical transition strain amplitude decreases dramatically to about 22% for PA1, for which the clay loading is as low as 1 wt %. On the basis of the results shown in Figures 3 and 4, we can conclude that the presence of nanometer-scale dispersed clay particles and individual layers is very sensitive to small strain; critical strain amplitudes deduced from both G' and G'' dramatically decrease, and the extent deduced from G'' is much more obvious than that deduced from G'. The reason may be briefly explained by the formation of a network comprising clay primary particles and individual layers. The presence of the anisotropic inorganic clay layers and primary particles increases G' and G''. Under strain amplitude, the clay layers and primary particles may be aligned in the flow direction, and this results in the lower critical strain transition of G' and G''.

Figure 5 shows the oscillatory sweep testing results measured by G' and G'' as a function of ω at 240°C. Compared with those of pure PA0, both G' and G'' of the nanocomposites (PA1) apparently increase. In addition, a low-frequency, solidlike behavior can be observed from the dynamic oscillatory responses, and the nanocomposite show more

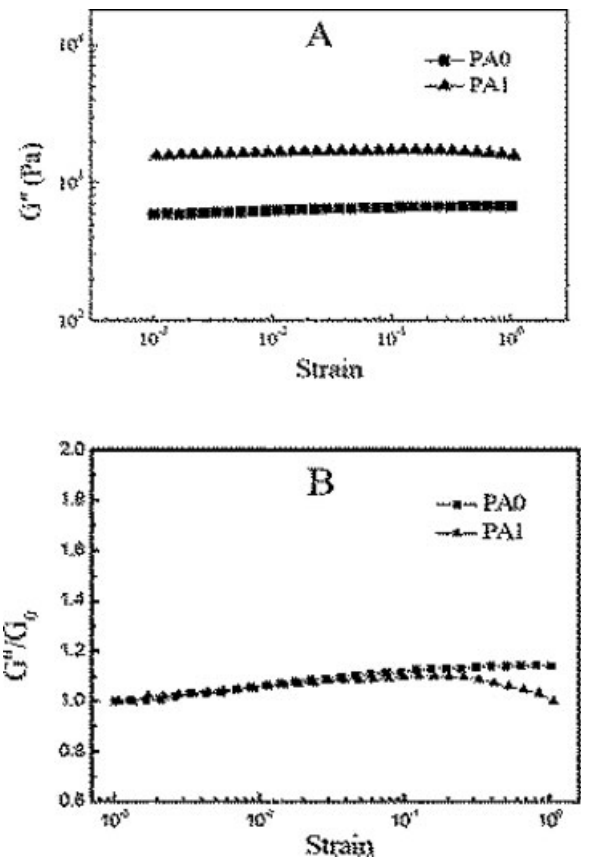

Figure 4 Strain amplitude dependence of (A) G'' and (B) G''/G_0 for PA1 and PA0 measured at 240°C.

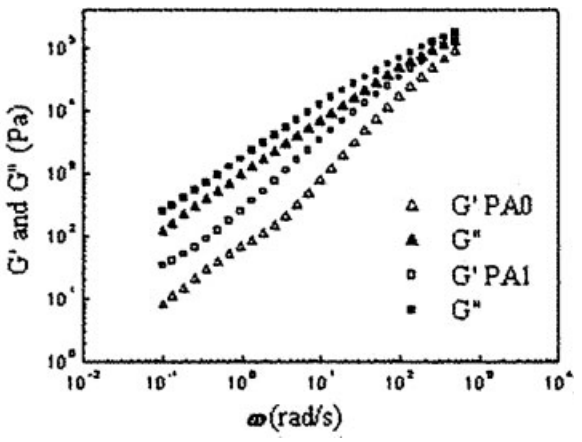

Figure 5 G' and G'' of PA1 and PA0 as a function of ω.

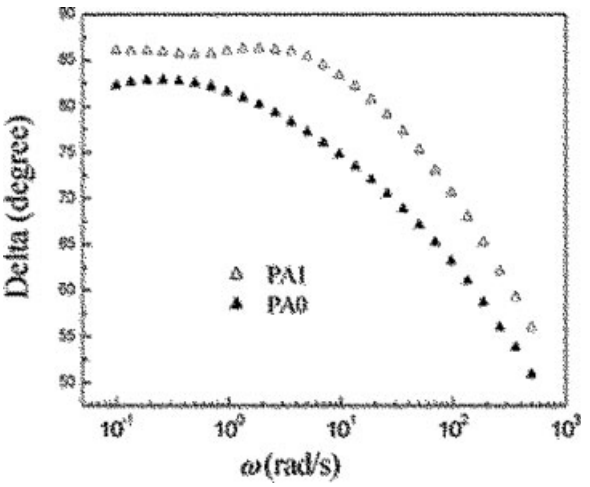

Figure 7 Loss angle of PA1 and PA0 as a function of ω.

pronounced solidlike behavior than neat PA0, with a decreased slope for G' and G'' of PA1.

The complex viscosity (η) during dynamic (0.1–500 rad/s) and steady (0.003–10 s^{-1}) shear rheological tests at 240°C is shown in Figure 6. η of PA1 is obviously higher than that of PA0, especially in the low shear rate region, whereas both exhibit shear-thinning behavior. This may be due to the dramatic exfoliation of clay into a nanometer-scale, homogeneous dispersion, as indicated by the aforementioned TEM image and WAXD pattern in Figures 1 and 2, and the strong interaction between clay and polymer chain segments. The shapes of the two curves are different, indicating that the clay layers and primary particles may contribute to the shear thinning. The clay may impede the entanglement mobility of polymer chains and modify the entanglement network when being sheared. According to the Cox–Maxwell equation, the zero shear rate viscosity (η_0) of PA0 was calculated to be 1464.72 Pa s.

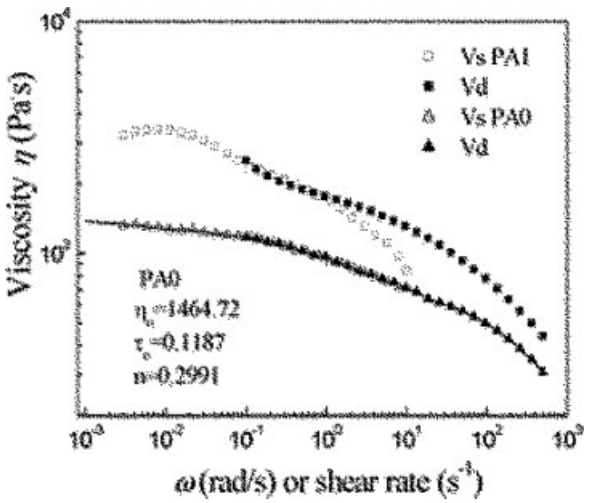

Figure 6 η of PA1 and PA0 as a function of ω or the shear rate during dynamic and steady shear tests.

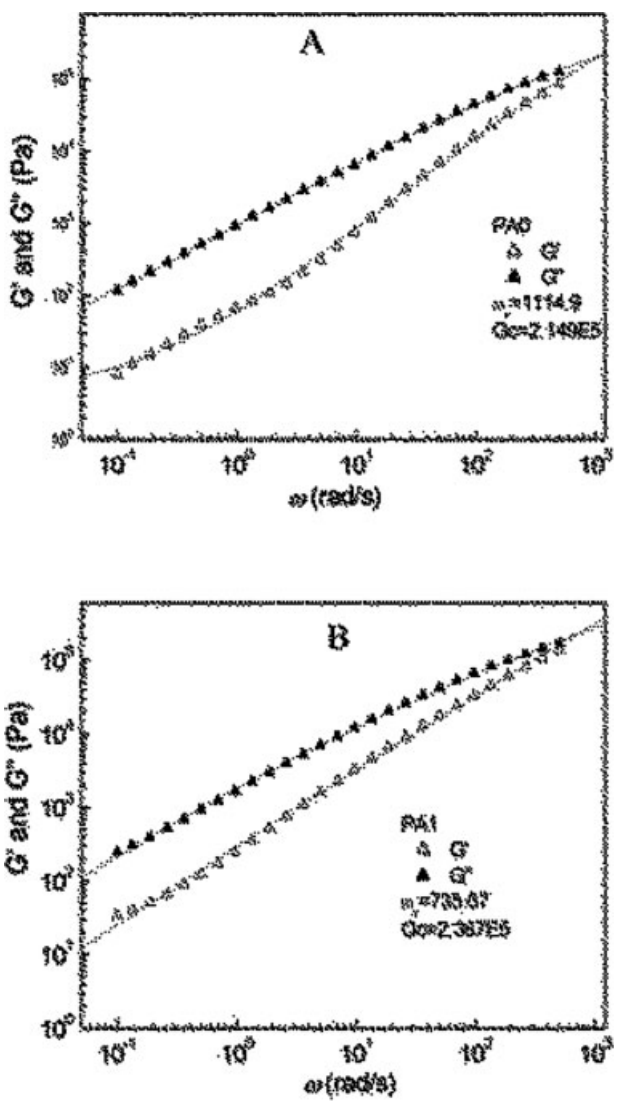

Figure 8 Plot of G' and G'' of (A) PA0 and (B) PA1 versus ω for measuring the intersection point.

Figure 7 shows the loss angles of PA0 and PA1. The loss angle of the nanocomposite (PA1) is obviously higher than that of PA0, suggesting the impediment of polymer chain mobility by MMT layers and primary particles. Because the nanocomposite of PA1 was synthesized by the *in situ* intercalative polymerization procedure, strong ionic bonds are prevalent at the interface between the PA6 chain segments and clay surface. In this case, the strong interfacial interaction will definitely impede the chain mobility during the shearing rheological tests, thus resulting in the increase of the loss angle.

Larson[15] compared G' and G'' for prototypical solidlike and liquidlike materials. Liquidlike behavior is characteristic for $G' < G''$, and solidlike behavior is expected when G' is greater than G'' and G' is almost independent of the frequency. Our data in Figure 7(A,B) show that the melt behavior is liquidlike for $G' < G''$. The values of the frequency and modulus at the intersection (ω_x and G_c, respectively) are calculated in Figure 8. ω_x of PA1 (735.67 rad/s) is obviously lower than that of PA0 (1114.9 rad/s). This is in accordance with the aforementioned loss angle results in Figure 7.

CONCLUSIONS

An obvious difference can be observed between the low-filled PA6/clay nanocomposite with only 1 wt % MMT and the neat PA6. The critical transition strain amplitudes for PA1, deduced from G' and G'', are obviously lower than those of the neat PA0. The nanocomposite exhibits an increase in G', G'', and η during the dynamic and steady sweep tests. Its loss angle increases and ω_x at the intersection of G' and G'' decreases in comparison with those of the neat PA6 matrix. The reason may be the dramatic exfoliation, homogeneous dispersion of the nanometer-scale clay primary particles and individual layers, and strong interfacial interactions between the polymer and clay. The clay layers and primary particles may impede the mobility of the polymer chains.

The authors are grateful for the rheological experimentation and helpful discussions of Ji Ping Yang and Chen Li of the School of Material Science and Engineering of Beihang University.

References

1. Wagener, R.; Reisinger, T. J. G. Polymer 2003, 44, 7513.
2. Médéric, P.; Razafinimaro, T.; Aubry, T.; Moan, M.; Klopffer, M. Macromol Symp 2005, 221, 75.
3. Aubry, T.; Razafinimaro, T.; Médéric, P. J Rheol 2005, 49, 425.
4. Hoffmann, B.; Kressler, J.; Stöppelmann, G.; Friedrich, C.; Kim, G. M. Colloid Polym Sci 2000, 278, 629.
5. Incarnato, L.; Scarfato, P.; Scatteia, L.; Acierno, D. Polymer 2004, 45, 3487.
6. Xu, Y.; Xu, Y. Chin J Polym Sci 2005, 23, 147.
7. Xu, L.; Reeder, S.; Thopasridharan, M.; Ren, J.; Shipp, D.; Krishnamoorti, R. Nanotechnology 2005, 16, 514.
8. Schmidt, G.; Nakatani, A. I.; Han, C. C. Rheol Acta 2002, 41, 45.
9. Wan, T.; Clifford, M. J.; Gao, F.; Bailey, A. S.; Gregory, D. H.; Somsunan, R. Polymer 2005, 46, 6429.
10. Tung, J.; Gupta, R. K.; Simon, G. P.; Edward, G. H.; Bhattacharya, S. N. Polymer 2005, 46, 10405.
11. Krishnamoorti, R.; Giannelis, E. P. Macromolecules 1997, 30, 4097.
12. Shen, L.; Lin, Y.; Du, Q.; Zhong, W.; Yang, Y. Polymer 2005, 46, 5758.
13. Karaman, V. M.; Privalko, V. P.; Privalko, E. G.; Lehmann, B.; Friedrich, K. Macromol Symp 2005, 221, 85.
14. Ayyer, R. K.; Leonov, A. I. Rheol Acta 2004, 43, 283.
15. Larson, R. G. The Structure and Rheology of Complex Fluids; Oxford University Press: New York, 1999.